Supporting Information

Shukla et al. 10.1073/pnas.1121174109

SI Text

Laminin Receptor Specific Therapeutic Gold Nanoparticles (^{198}AuNP-EGCg) Show Efficacy in Treating Prostate Cancer. ***Materials and methods.*** 18-MΩ/cm^2 water was obtained in-house from a MilliQ water filtration system (Millipore Corp., Billerica, MA). All other chemicals and reagents that were used were procured from commercial vendors and used without further purification. Transmission electron Microscope (TEM) images were obtained on JEOL 1,400 transmission electron microscope (TEM), JEOL, LTD., Tokyo, Japan. TEM samples were prepared by placing 5 μL of gold nanoparticle solution on the 300 mesh carbon coated copper grid and the solution was allowed to sit for 5 min; excess solution was removed and the grid was left to dry for an additional 5 min. The average size and size distribution of gold nanoparticles synthesized in this work were determined by detailed analysis of TEM images using image processing software such as Adobe Photoshop (with Fovea plug-ins). The absorption measurements were carried out using Varian Cary 50 UV-Vis spectrophotometers with 1 mL of gold nanoparticle solution in disposable cuvettes of 10 mm path length. Size and surface charge of gold nanoparticles were measured by Dynamic light scattering (DLS, Malvern Zetasizer) techniques. Missouri University Research Reactor (MURR) irradiation facilities were used for the production of Au-198 using high purity gold foil targets.

Characterization and in vitro stability of EGCg-AuNPs. The surface plasmon resonance wavelength, λ_{max}, and plasmon band width, $\Delta\lambda$, of EGCg-AuNPs are approximately 535 nm and 65 nm, respectively, indicating the formation of EGCg-AuNP (Fig. S1*A*) (1). The core size of the EGCg-AuNP is 40–55 nm, as determined from TEM images (Fig. S1*B*), while the hydrodynamic radius revealed that 95% of EGCg-AuNP conjugates have an average diameter of 120–130 nm (Fig. S1*C*). This implies that the EGCg coating over AuNP occupies approximately 85 nm. The zeta potential is an indication of repulsive forces that are present in aqueous solution and can be used to predict the long-term in vitro/in vivo stability of nanoparticulate dispersions. The high zeta potential of −37.7 mV as observed for EGCg-AuNP is a clear indication of its high stability against aggregation (Fig. S1*D*) (2).

The stability of EGCg-AuNP was evaluated in various biological fluids to establish its intended utility under in vivo conditions. Solutions of EGCg-AuNP were challenged with 10% NaCl, 0.2 M histidine, 0.5% human serum albumin (HSA), 0.5% Bovine Serum Albumin (BSA) and at various pH values (7, 9) and the stability was monitored through changes in surface plasmon resonance (λ_{max}) and plasmon band width ($\Delta\lambda$) (Fig. S2). The λ_{max} and $\Delta\lambda$ in all of the above media shifted by only approximately 10 nm, indicating excellent in vitro stability. Further in vitro stability of EGCg-AuNPs was assessed by incubating the nanoparticles in cell culture media. No detectable aggregation/decomposition was noted in these experiments (Fig. S2). The non-radioactive EGCg-AuNPs were determined to be stable at room temperature without any noticeable aggregation over a period of 12 months when stored at 25 °C in closed vials. The in vitro studies have validated stability of EGCg-AuNPs in biological fluids at physiological pH suggesting that EGCg coating provides a robust shielding around AuNPs, thus rendering in vitro stability. It is significant to note that no additional capping agent was used during the synthesis of EGCg-AuNPs, indicating that the FDA approved phytochemical EGCg serves as both a reducing and capping agent to produce in vitro and in vivo stable AuNPs.

Synthesis of ^{198}AuNP-EGCg. Gold leaf (0.76 mg) was irradiated for 3.5 h. The calculated activity of ^{198}Au was 20.5 mCi according to the Capintec® CRC-12. The ^{198}Au foil was placed in a Liquid Scintillation Counting (LSC) vial and dissolved in 800 μL of aqua regia. The solution was heated to reduce the volume to approximately 200 μL. Then 600 μL of 0.05 M HCl was added and heating continued until most of the acid had evaporated. The solution was removed from the hot plate and allowed to cool followed by the addition of 200 μL of 0.05 M HCl. A 0.17 mg/mL solution of EGCg was prepared in Milli-Q water and stirred continuously at 25 °C for 3 min. To the stirring mixture was added 2 μL of H^{198}AuCl$_4$ (0.41–1.3 mCi) and 98 μL of 0.1 M NaAuCl$_4$ carrier solution. The color of the mixture turned purple-red from pale yellow within 5 min indicating the formation of gold nanoparticles. The reaction mixture was stirred for an additional 15 min at 25 °C. The UV-Vis spectrometer was used to characterize ^{198}AuNP-EGCg (Fig. S3). The homogeneous distribution of nanoparticles in ^{198}AuNP-EGCg was ascertained by observing the Plasmon absorption band and the band width. The formation of AuNP was monitored through a color change from yellow to purple red. Solutions were evaluated by spectrophotometry on an Ocean Optics USB2000 to confirm the formation of ^{198}AuNP-EGCg. The change in color from pale yellow to purple red is diagnostic of a plasmon-plasmon transition present in gold nanoparticles. The plasmon absorption band at 535 nm with the width of 90 nm was considered as homogeneous distribution.

In order to ascertain the percent conversion of ^{198}AuCl$_4^-$ to nanoparticles, standard thin layer chromatography technique was used to differentiate the unreacted ^{198}AuCl$_4^-$ from the ^{198}AuNPs. A radiochemical purity and percent labeling was tested by TLC on Whatman cellulose paper. Briefly: 3 μL of the solution was spotted onto Whatman cellulose plates and developed in methanol (2 mL) with 1 drop of concentrated HCl (approximately 10 M). The paper strip was scanned on a BioScan to determine the percent radiolabeling yield. The ^{198}AuNP-EGCg functionalized nanoparticles remains at the origin $R_f = 0$, and free ^{198}AuCl$_4^-$ migrates with an R_f of 0.9. The radiolabeling yield was >99% (Fig. S3).

Hemocompatibility studies. Hemolytic studies were used to assess the biocompatibility of nanoparticles by direct exposure to freshly drawn human blood from healthy volunteers. The nanoparticles were tested for hemolysis and a quantitative colorimetric assay for hemoglobin release was performed. Briefly, fresh blood from two human volunteers was drawn, collected in CPD (Citrate Phosphate Dextrose) solution and due care was taken for thorough mixing to achieve homogeneity. The cells were thoroughly washed with veronal buffered saline (VBS) containing 5 mM barbital and 145 mM NaCl (pH 7.4). After 3–4 washes, when the supernatant was clear, the packed RBCs fraction was adjusted by diluting in such a way that RBC lysate in water gave an optical density (OD) of 1 at 405 nm. The adjusted RBC solution was kept on ice and was used in duplicates by mixing 10 μL of RBC suspension with increasing concentrations of EGCg-AuNP and the final volume of each tube was adjusted to 100 μL by addition of VBS. The tubes were incubated at 37 °C for 2 h with occasional mixing by gentle tapping. RBC lyses in water was considered 100% while in VBS was considered 0%. After incubation, 200 μL of VBS buffer was added to each tube and centrifuged at 3000 rpm for 2 min in a refrigerated centrifuge. A 100 μL aliquot of supernatant from each tube was added to each of 96 well ELISA plate in duplicates and the extent of RBC lyses

determined at 405 nm in Spectra Max plate reader (Molecular Device, USA).

Hemocompatibility assessment of EGCg-AuNP. Nontoxic and favorable biocompatibility characteristics of nanomaterials are important considerations in the context of their utility for biomedical applications. EGCg is a catechin abundantly found in green tea and forms a biologically favorable and stable matrix around gold nanoparticles. It is therefore expected that EGCg-AuNP conjugates are biocompatible. We have evaluated the dose dependent hemocompatibility of EGCg-AuNP in human blood (Fig. S4). The hemocompatibility assay involved direct exposure of EGCg-AuNP to freshly drawn whole human blood for 2 h at 25 °C. The results obtained from the hemocompatibility studies confirmed that ≥92% of the RBCs, upon exposure to various concentrations of EGCg-AuNP, remained intact, indicating the suitability of the EGCg-AuNPs for various molecular imaging and therapy applications. The hemocompatibility data are presented in Fig. S4. These studies suggest that EGCg-AuNP has favorable hemocomptability.

Quantitative RT PCR analysis of Lam 67R expression. Isolation of RNA was performed using RNeasy kit and established procedures following the manufacturer's instructions (Qiagen, Inc. USA. Valencia, CA). RNA was treated with RNase-free DNase and reverse transcribed by using SuperScript® III Reverse Transcriptase kit (Invitrogen, USA). Calf Thymus DNA (cDNA) was synthesized from 1 μg of total RNA using oligo dT primers provided in a kit following the manufacturer's instructions. Quantitative RT-PCR was achieved by cDNA (250 ng/reaction) amplification in the presence of the DNA-binding dye absolute QPCR SYBR Green Fluorescien mix (Thermo Scientific, USA) and forward and reverse primers. The following primer pairs were used for Lam 67R (5′-TCACTCAGTGGGTTTGATGTG-3′ and 5′-TTCAGACCAGTCTGCAACCTC-3′) and HPRT [hypoxanthine phosphoribosyl-transferase] (5′-GCTGGTGAAAAGGACCTC-T-3′ and 5′-CACAGGACTAGAACACCTG-3′)]. Relative quantitation of Lam 67R expression in U266 and PC-3 cells was performed by using the comparative Ct method. The Ct value was defined as the cycle number at which the PCR amplification graph passed a threshold, which was calculated by the maximum curvature approach and set to be 376.4 for the experiment. The amount of targets and endogenous reference HPRT was determined from the standard curve. Next, the target values were normalized to the endogenous reference, assuming that HPRT expression was identical in the different samples. The relative amount of Lam 67R mRNA was calculated by using the formula: $2^{-\Delta\Delta Ct}$, where $\Delta\Delta Ct = [Ct_{target} - Ct_{HPRT}]_{mutant} - [Ct_{target} - Ct_{HPRT}]_{wildtype}$. For U266 cells, ΔΔCt equals zero and 2° equals one. For PC-3 cells, the value of $2^{-\Delta\Delta Ct}$ indicates the fold change in gene expression relative to the U266 control cells. The level of Lam 67R expression on PC-3 cells and U266 control cells monitored through quantitative RT-PCR is presented in Fig. S5.

Determination of internalized gold in PC-3 cells due to endocytosis of EGCG-AuNP by neutron activation analysis (NAA). Human prostate cancer cell line PC-3 was obtained from the American Type Culture Collection (ATCC; Manassas, VA), and cultured according to ATCC recommendations by the University of Missouri Cell and Immunobiology Core facility. The actively growing PC-3 cells (2.5×10^5 cells/mL) were seeded in 100 mm tissue culture plates and allowed to grow till 70% confluency was achieved. These cells were treated with 30 μg/mL of EGCg-AuNP. The cells were incubated with gold nanoparticle for 90 min and then were washed thoroughly with plain medium followed by an excess of PBS a total of 10 times. Before trypsinization, cells were given a brief wash with PBS containing 0.1 M HCl. The cells were dislodged using triple E (Invitrogen) solution and the resulting cell suspension was washed with ice cold PBS a total of three times. After the final washing, cells were fixed with 75% ethanol and the cell pellet was dehydrated with several changes of 1 mL absolute ethanol at 60 °C. After five rounds of ethanol wash, the dehydrated pellet was weighed and subjected to NAA analysis.

Sample preparation for NAA. Samples were prepared by placing the cell pellet (dry weight) into pre-cleaned, high-density polyethylene irradiation vials. The weight of each sample was recorded and the vial was capped. Blanks, duplicates, and spiked samples were included in the NAA sample sets.

NAA analysis. Samples were loaded in polyethylene transfer "rabbits" in sets of nine and were irradiated for 90 s in a thermal flux density of approximately 5×10^{13} n/cm^2/s. The samples were then allowed to decay for 24–48 h and counted in real time for 1,200 s at a sample-to-detector distance of approximately 5 mm. The spectrometer consisted of a 21% high-purity germanium detector, with a full-width-at-half-maximum resolution of 1.8 keV at 1331 keV, and a Canberra 9660 digital signal processor. Dead times ranged from 1 to 11%. The mass of gold was quantified by measuring the 411.8 keV gamma ray from the β^- decay of ^{198}Au ($t_{1/2} = 2.7$ days). The area of this peak was determined automatically with the Genie ESP spectroscopy package from Canberra. Nine geometrically equivalent comparator standards were prepared by pipetting approximately 0.1 mg of gold from a (10.0 ± 0.5) μg/mL certified standard solution (High-Purity Standards) on paper pulp in the polyethylene irradiation vials. Analysis of the gold comparator standards yielded a relative specific activity (average and standard deviation) of (237239 ± 6084) counts/μg Au ($n = 9$) with a relative standard deviation of 2.6%.

Sample preparation for transmission electron microscopy. After treatment with EGCg-AuNPs, tumor cells were extensively washed, dislodged, pelleted, and fixed with 0.1 M sodiumcacodylate buffer containing 2% glutaraldehyde and 2% paraformaldehyde. The pellets were post fixed with 1% osmium tetraoxide, dehydrated and embedded in Epon/Spurr's resin and 80 nm sections were collected and placed on electron microscopy (EM) grids followed by sequential counter staining with urenyle acetate and lead citrate. The grids were observed under Transmission Electron Microscope (TEM) (Joel 1400) and images were recorded at different magnifications.

Biodistribution and tumor retention capabilities of ^{198}AuNP-EGCg. Animal studies were approved by the Institutional Animal Care and Use Committees (IACUC) of the Harry S. Truman Memorial Veterans Hospital and the University of Missouri, and were performed in accordance with the Guide for the Care and Use of Laboratory Animals. Female ICRSC-M SCID mice (4–5 wk of age; Taconic Farms, Hudson, NY) were group housed on a 12 h light-dark cycle in a pathogen-free barrier facility having controlled temperature and humidity. Animals had access to sterilized standard chow and water ad libitum, and were acclimated for 7–10 d prior to manipulations. The PC-3 human prostate cancer cell line was obtained from the American Type Culture Collection (ATCC; Manassas, VA), and cultured by the University of Missouri Cell and Immunobiology Core facility using procedures recommended by ATCC. To monitor the tumor retention capabilities, we have performed intratumoral (IT) injections of ^{198}AuNP-EGCg nanoparticles in severely compromised immunodeficient (SCID) mice bearing bilateral flank tumor xenografts of human PC-3 prostate cancer.

Mice received bilateral subcutaneous hind flank inoculations of 10×10^6 PC-3 cells (passage 20) suspended in 0.1 mL of sterile

Dulbecco's phosphate buffered saline (DPBS) and Matrigel® (2:1, v:v) under inhalational anesthesia (isoflurane/ oxygen). Solid tumors were allowed to develop for four weeks, and animals were randomized into five groups ($n = 5$). Animals in each group received intratumoral (*i.t.*) injections of ^{198}AuNP-EGCg (3.5 μCi) in DPBS (20 μL) while under brief inhalational anesthesia. Groups were euthanized by cervical dislocation at intervals of 30 min, 1, 2, 4 and 24 h. Analysis of ^{198}Au radioactivity revealed that $72.4 \pm 5.9\%$ ID (mean ± sem, $n = 5$) of ^{198}AuNP-EGCg nanoparticles was retained in prostate tumors at 24 h, and was nearly constant from 30 min (77.8 ± 5.5) to 24 h. The ^{198}AuNP-EGCg nanoparticles exhibited slow clearance (leakage) into the blood with only 0.06% ID/g at 24 h. Lungs and pancreas exhibited low uptake at 24 h with only 0.33% ID/g and 0.22% ID/g, respectively. The uptake in the stomach peaked at 5% ID/g at 2 h and decreased to 0.03% ID/g at 24 h. The highest uptake in the small intestines was observed at 2 h with 0.91% ID/g that reduced to 0.01% ID/g at 24 h. The kidneys and spleen showed slow uptake over time with 0.12% ID/g and 1.56% ID/g at 24 h. The liver had 0.51% ID/g after 30 min and increased to 6.13% ID/g after 24 h. The gastrointestinal uptake mentioned above contributed to the feces having 1.71% ID after 24 h. Blood samples were obtained by cardiac puncture. Urine and feces were collected from cage papers representing the entire time interval. Tumors and organs of interest were harvested, weighed and then counted using an automated γ-counter to determine the percent injected dose per gram (%ID/g) and per organ at each time. Mean tumor weights for the five groups ranged from 0.18 to 0.23 g, with no significant differences ($p > 0.05$, ANOVA) between groups. These pharmacokinetic features confirmed excellent retention of therapeutic payloads of ^{198}AuNP-EGCg nanoparticles within prostate tumors with only minor leakage to non-target organs.

Blood parameters for therapeutic efficacy. Blood parameters were compared between the ^{198}AuNP-EGCg treatment ($n = 6$), EGCg control ($n = 6$) and saline control ($n = 7$) groups with baseline levels obtained from a fourth group ($n = 7$) of normal SCID mice that received no manipulations. One blood sample from the non-radioactive EGCg group clotted, and was excluded from analysis. Blood from all animals euthanized in mid-study were analyzed immediately, and those values were included with data from animals euthanized at the end-of-study. Analysis of variance showed no significant differences ($p > 0.05$) between any of the groups for any blood parameters (Fig. S6).

Control experiments. The importance of EGCG coating is clearly evident by comparing the retention and therapeutic efficacy data of our previously reported gum arabic stabilized radioactive gold nanoparticles (GA-^{198}AuNP) (3). Gum Arabic is a glycoprotein and is not known to have affinity towards Lam-67R receptor present in prostate tumor cells and therefore, GA-^{198}AuNP serves as an excellent control agent for comparison of in vivo therapeutic efficacy characteristics with those of ^{198}AuNP-EGCg. The natural affinity of EGCg towards Lam-67R receptors, overexpressed in prostate cancer cells (PC-3), is well recognized in the literature (4). After confirming the receptor affinity of EGCg in PC-3 cells, conjugation of EGCg with gold nanoparticles (40–55 nm) at room temperature was explored (for full details on receptor specificity, see the section *Laminin-67 Receptor Mediated Cellular Internalization of EGCg-AuNP*, Fig. 1 *A*–*2D*; Lam67-R expression in PC-3 cells as shown in Fig. S5). EGCg has several advantages of being a reducing, stabilizing, and targeting agent. We hypothesized that the receptor recognition combined with the larger size would result in a higher retention of ^{198}AuNP-EGCg compared to the control GA-^{198}AuNPs. As shown in Fig. S7, the intratumoral injections of gold nanoparticles did not show major differences in retention characteristics between GA-^{198}AuNPs and ^{198}AuNP-EGCgs at 30 min post injection. However, at 24 h post injection, a significant difference in retention was observed. ^{198}AuNPs-EGCg was retained in tumors for a significantly longer time period compared to GA-^{198}AuNPs (Fig. S7). This longer retention of ^{198}AuNP-EGCg allowed us to inject only a third of the activity of ^{198}AuNP-EGCg (136 mCi for ^{198}AuNP-EGCg vs. 408 mCi for GA-^{198}AuNPs) and achieve comparable results in tumor reduction with time. The results of the control experiments as depicted in Fig. S7 provide compelling evidence that the retention characteristics of ^{198}AuNP-EGCg are superior as compared to GA-^{198}AuNP and thereby highlight the importance of conjugating AuNPs with the Lam-67R receptor specific EGCg.

1. Kattumuri V, et al. (2007) Gum arabic as a phytochemical construct for the stabilization of gold nanoparticles: In vivo pharmacokinetics and X-ray-contrast-imaging studies. *Small* 3:333–341.
2. Nune SK, et al. (2009) Green nanotechnology from tea: Phytochemicals in tea as building blocks for production of biocompatible gold nanoparticles. *J Mater Chem* 19:2912–2920.
3. Chanda N, et al. (2010) Radioactive gold nanoparticles in cancer therapy: Therapeutic efficacy studies of GA-198AuNP nanoconstruct in prostate tumor-bearing mice. *Nanomedicine* 6:201–209.
4. Tachibana H, Koga K, Fujimura Y, Yamada K (2004) A receptor for green tea polyphenol EGCG. *Nat Struct Mol Biol* 11:380–381.

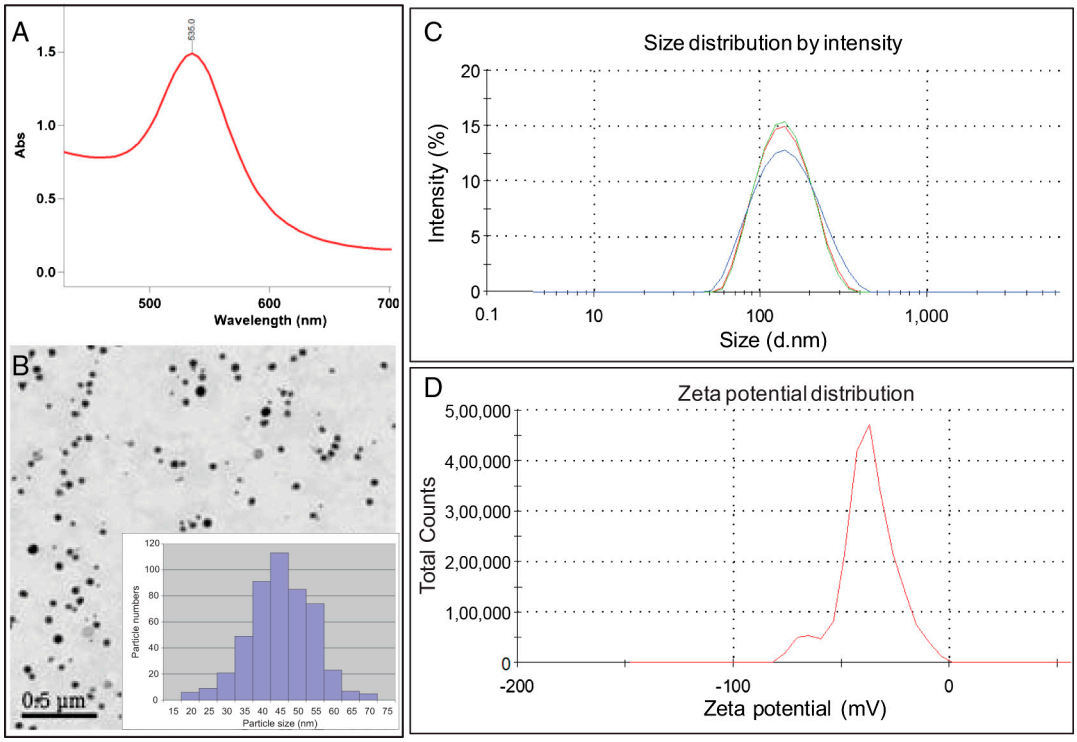

Fig. S1. Physico-chemical characterization of EGCg-AuNP (*A*) UV-Visible spectra, (*B*) TEM Image, (*C*) hydrodynamic size measured from three different batches of nanoparticles, and (*D*) Zeta-potential distribution. *Inset* in (*B*) shows the core size distribution of particles.

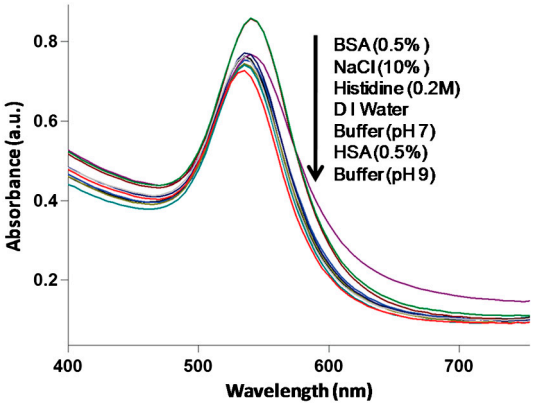

Fig. S2. In vitro stability of EGCg-AuNP in various media. The nanoparticles were exposed with aqueous solutions of BSA (0.5%), HSA (0.5%), NaCl (10%), Histidine (0.2 M), and different pH buffers (7 and 9) for 60 min and the UV-Vis spectra were recorded.

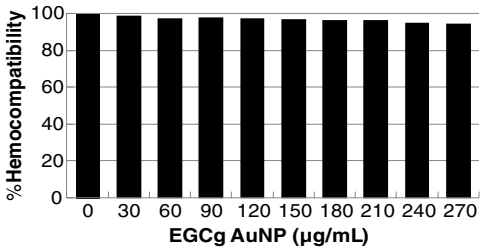

Fig. S3. Hemocompatibilty of EGCg-AuNPs. Increasing concentrations of nanoparticles were incubated with human red blood cells for 2 h. Extent of RBC lysis was calculated against DI water considering 100% lysis.

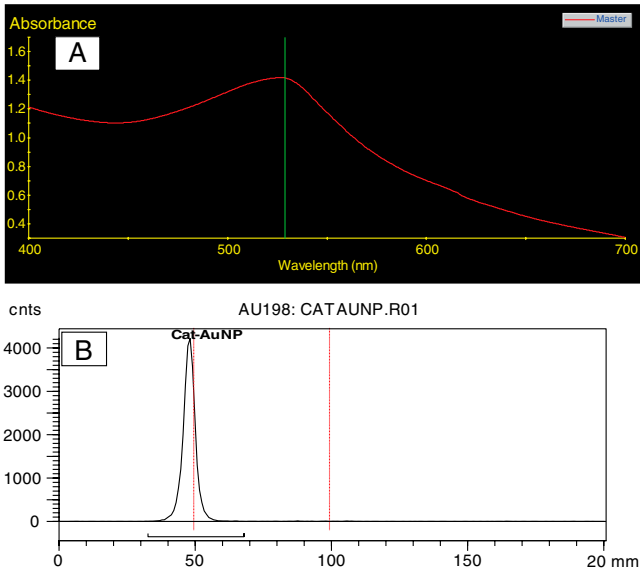

Fig. S4. Physico-chemical characterization of ^{198}AuNP-EGCg. (*A*) UV-Visible spectra and (*B*) Bioscan analysis of a radio-thin layer chromatograph of ^{198}AuNP-EGCg.

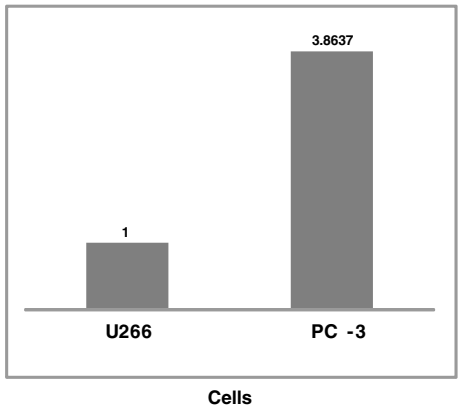

Fig. S5. Laminin 67R expression in PC-3 cells at RNA level is evident by real time PCR wherein U266 cells were used as control cells for basal level of Lam-67 R expression.

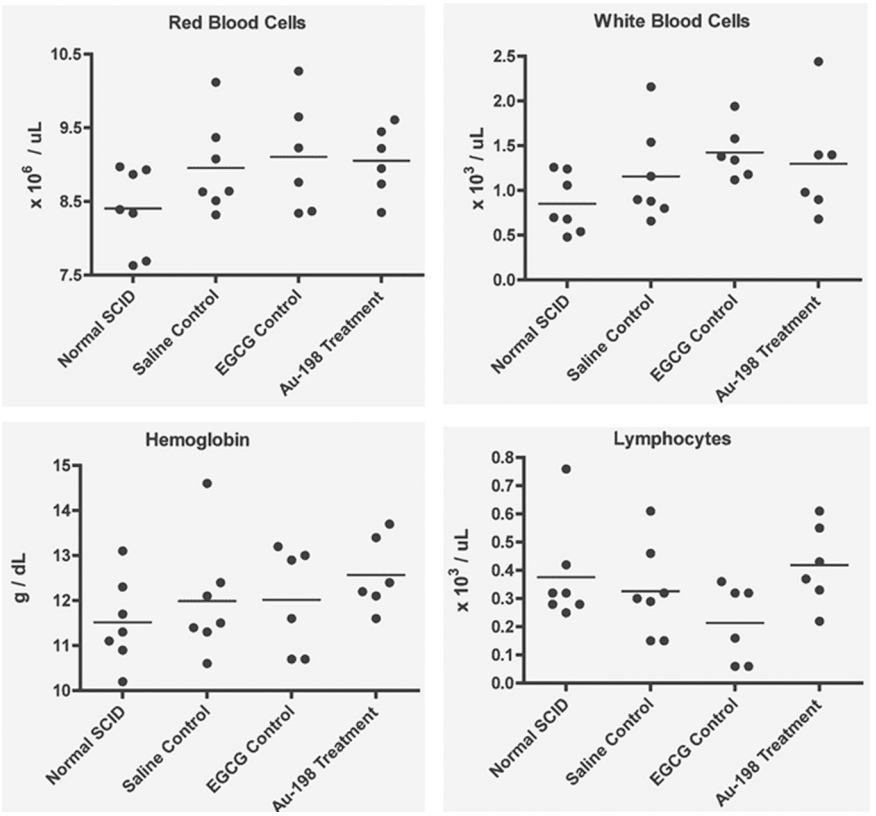

Fig. S6. Comparison of blood parameters including: (*A*) RBCs, (*B*) WBCs, (*C*) hemoglobin, and (*D*) lymphocytes between the ^{198}AuNP-EGCg treatment ($n = 7$), EGCg ($n = 6$) control, and saline control ($n = 7$) groups with the baseline levels obtained from a fourth group of normal SCID mice ($n = 7$) that received no manipulations.

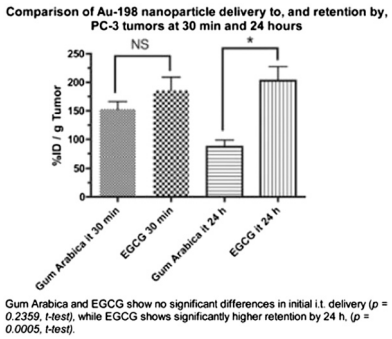

Fig. S7. Comparison of GA-^{198}AuNP and ^{198}AuNP-EGCg retention (%ID/g) at 30 min and 24 h time post injection time points in PC-3 tumor bearing in SCID mice model.